



# Determination of sedimentation rates and life of Kodaikanal Lake, South India, using radiometric dating ( $^{210}\text{Pb}$ and $^{137}\text{Cs}$ ) techniques

Balamurugan Palani<sup>1</sup> · Sivaprakasam Vasudevan<sup>1</sup> · Thirunavukkarasu Ramkumar<sup>1</sup> · Selvaganapathi Rajendiran<sup>1</sup> · Sathyamoorthy Gunasekaran<sup>1</sup>

Received: 29 March 2022 / Accepted: 6 April 2023 / Published online: 25 April 2023  
© The Author(s), under exclusive licence to Springer-Verlag GmbH Germany, part of Springer Nature 2023

## Abstract

A study describes the use of natural ( $^{210}\text{Pb}$ ) and anthropogenic ( $^{137}\text{Cs}$ ) radiometric dating techniques to determine sedimentation rates and age of Kodaikanal Lake. The core sediment from 46 cm was collected and analyzed for  $^{210}\text{Pb}$  and  $^{137}\text{Cs}$  using an Alpha spectrometer 7200-04 and a Gamma-ray spectrometer GC-3520. Bathymetry studies aided in selecting a representative sample location and measuring the lake's underwater depth, with maximum and mean depths of 11 and 3.38 m, respectively. The maximum and minimum dry bulk density ranged from 0.57 to 1.05 g/cm<sup>3</sup> (mean of 0.73 g/cm<sup>3</sup>), and the weight percentage of porosity collected sediment sample ranged from 60.33 to 78.63 wt.% (mean of 72.32 wt.%). This study determined the sediment grain size and the percentages of sand, silt, and clay. The findings indicate that the core sediment samples contain 56.05 to 69.62 wt.% (mean of 63.21 wt.%) sand, 28.03 to 41.71 wt.% (mean of 34.55 wt.%) silt, and 1.81 to 3.98 wt.% (mean of 2.34 wt.%) clay. The  $^{210}\text{Pb}$  technique was used to assess a model of time changes in the deposit for geochronology studies in core sediments. The sedimentation rate depended on the consistent rate supply (CRS) of the  $^{210}\text{Pb}$  model. The  $^{210}\text{Pb}$  model was confirmed using  $^{137}\text{Cs}$  radioactivity released into the global fallout after nuclear testing (1963) and the Chernobyl accident (1986). The depth concentration of  $^{210}\text{Pb}$  ranged from  $3.89 \pm 0.1$  to  $15.4 \pm 1.6$  Bq/kg, with a mean of  $7.23 \pm 0.86$  Bq/kg. The  $^{137}\text{Cs}$  radioactivity varied from the upper and lower peaks that appeared clearly at depths of 16 and 29 cm, respectively, with successive phases of  $18.68 \pm 1.36$  and  $22.04 \pm 1.4$  Bq/kg. According to the CRS model, the mean sedimentation rate was  $0.51 \pm 0.14$  cm/year, and the core age was 86 years. The  $^{137}\text{Cs}$  have likely been the mean sedimentation rate of  $0.535 \pm 0.07$  cm/year and 83 years. The evaluated life of Kodaikanal Lake as an average of  $^{210}\text{Pb}$  and  $^{137}\text{Cs}$  sedimentation rate since 1933 is about  $650 \pm 24$  years and  $582.75 \pm 19$  years.

**Keywords** Sedimentation rates · Life of Kodaikanal Lake · CRS model ·  $^{210}\text{Pb}$  and  $^{137}\text{Cs}$  dating techniques

## Introduction

Sediments consist of particles transferred by water, wind, and moving ice from their origins in the terrestrial environment and deposited on the open sea, lakes, and rivers. Geological structure, geomorphological features, morphometric character, and climatic conditions influence the chemical composition of sediments. Undefined, the watershed or lake location significantly impacts the constitution of sediment (Last and Smol 2001; Szarlowicz et al. 2017). Sediments can also represent trace metals, organic materials, radioactive

isotopes, and other contaminants. Hence, they serve as natural pollutant storage facilities and are essential in distributing environmental pollutants in aquatic environments (de Deckere et al. 2011; Grba et al. 2016; Szarlowicz et al. 2017).

The radioactivity source has proven to be an effective tool in the environmental study for determining the sedimentation rates using natural ( $^{210}\text{Pb}$ ) and anthropogenic ( $^{137}\text{Cs}$ ) processes in our environment. The decay sequence of  $^{238}\text{U}$  is a natural source of radionuclides with a half-life of 22.3 years (Appleby 2008). It is sensitive to the dating of various environments such as soil, sediment, glaciers, coral reefs, wetlands, and peatlands for 100–150 years (Appleby et al. 1997; Baskaran et al. 2014; Simon et al. 2017; Singh and Vasudevan 2021) of the ocean and marine assessments as well as estimates of atmospheric fallouts, sedimentation, and pollution (Baskaran 2011; Bikit et al. 2004; Jeter 2000;

✉ Balamurugan Palani  
palanibala2@gmail.com

<sup>1</sup> Department of Earth Sciences, Annamalai University, Annamalai Nagar 608 002, India

Sanders et al. 2006, 2011; Singh and Vasudevan 2021). The decay product of radium-226 ( $^{226}\text{Ra}$ ), a number of the uranium chain ( $^{238}\text{U}$ ), produces  $^{222}\text{Rn}$  in rocks, soil, and sediments. A portion of radon atoms is released into the environment by decaying  $^{226}\text{Ra}$  in the soil to  $^{210}\text{Pb}$  into a series of short-lived isotopes. Since  $^{210}\text{Pb}$  has a shorter time to recover in the atmosphere, it is rapidly deposited in sediment and becomes permanently bound to sediment particles in just a few months (Tee et al. 2003; Guo et al. 2020; Sun et al. 2020). Therefore, it is essential to find a core sediment chronology by measuring the surface activity of the core sediment and subsequent samples at regular intervals (relative to the surface). The radionuclide source has been widespread and is often used to determine constant chronologies of sedimentation rates and pollution loads over a dating horizon of seven half-lives, or 120 to 150 years (Kirchner 2011; Corcoran et al. 2018).

Among these artificial radionuclides, the long-lived  $^{137}\text{Cs}$  contribute significantly to radioactive effluence in aquatic ecosystems. It is essential due to its vast mass production during nuclear fission events and longer half-life (30.07 years) than other radiocesium isotopes like  $^{134}\text{Cs}$  (half-life of 2.06 years). There are numerous  $^{137}\text{Cs}$  sources in the environment. The atmospheric nuclear weapon tests of the 1950s and 1960s accounted for a significant source of the fallout in 1963 (Carter and Moghissi 1997; UNSCEAR 2000; Tsabaris et al. 2012). In addition, nuclear accidents have significant consequences for people, the environment, or the facility; the Chernobyl Accident (CA) and the Fukushima Daiichi Nuclear Power Plant (FNPP) are the current environment's significant sources of  $^{137}\text{Cs}$ . The Chernobyl disaster occurred on Saturday, April 26, 1986, at the Chernobyl Nuclear Power Plant's No. 4 reactor near Prip'yat in the Soviet Union's Ukrainian SSR (Burgherr et al. 2008; Chernobyl Nuclear Accident 2014). The FNPP disaster occurred on March 11, 2011, in Sendai, Miyagi Prefecture, on the eastern coast of Honshu Island (Japan's central part), as an effect of the tsunami caused by the Tohoku earthquake. It contributed to increased radioisotope emanation into the environment (Szefer 2002; Al-Masri et al. 2003; HELCOM 2003; Butler 2011; Chino et al. 2011).

The  $^{210}\text{Pb}$  and  $^{137}\text{Cs}$  were employed to estimate the ages of core samples taken from the different aquatic environments (McCall et al. 1984; Ritchie and McHenry 1990; Walling and He 1992; Aycik et al. 2004; Klaminder et al. 2012; Szczepanska et al. 2012). The main objective of the research is to evaluate the presence of  $^{210}\text{Pb}$  in sediment cores and its utility in assessing sedimentation rates and the life of Kodaikanal Lake. We will also briefly examine the probability of using  $^{137}\text{Cs}$  fallout from nuclear testing for the same purpose. The increasing trend in sedimentation rate in the small lake may make short periods of lake sedimentation and degrade the aesthetic quality of the aquatic environment.

Furthermore, the side effect of development influences the local economy by raising the costs of lake restoration and retarding tourism development (Torabi Kachosangi et al. 2020).

Lake management improvement is the guarantee of determining current conditions and predicting potential developments. The anticipated sedimentation rates would make future palaeoenvironmental and palaeoclimatic investigations on mountain lakes possible. These studies would also help understand the productivity and life of these lakes under normal environmental conditions.

## Study area

The Kodaikanal Lake is a freshwater Lake, and it's located in the Dindigul district, South India, in the Western Ghats region of the Palani Hills. This lake is a star-shaped deep blue lake amid lush evergreen slopes, and it is an artificial lake located in Kodaikanal's heart, perched at an elevation of 2130 m above sea level. It is a closed basin with approximately 24 hectares and is situated north of the thermometer factory. The lake is the most well-known geographical feature and tourist attraction in Kodaikanal. It lies between lake latitudes of N 10° 13' and N 10° 14' and the longitudes of E 77° 28' and E 77° 29' (Fig. 1).

The climate in Kodaikanal is semi-arid, with highs of 24 °C and lows of 13 °C in the summer (April and May) and highs of 16 °C and lows of 7 °C in the winter (December and January). The annual rainfall in the Kodaikanal Lake catchment is 1650 mm, and the rainfall record shows that heavy precipitation occurs in April, October, and November. It receives rainfall during both monsoons, with the northeast monsoon bringing the most.

## Materials and methods

### Bathymetry

The water depth in Kodaikanal Lake was calculated with a Garmin GPS Map-178 (chart plotter/sounder) equipped with a dual-frequency 50/200 kHz transducer for offshore boating and a single-frequency 200 kHz transducer for inland lakes and shores. The Garmin GPS Map-178 chart plotter/sounding eco-sounder has an integrated GPS that permits simultaneous depth and coordinate data logging. The surface of lake depth was measured the number of times for each second along with the logging pathways points (Szarlowicz et al. 2017). The found dataset includes depth measurements and coordinates from the global positioning system (GPS). The bathymetry model uses ESRI software's spatial analyst extension available in ArcGIS 10.1. The spatial analyst tool

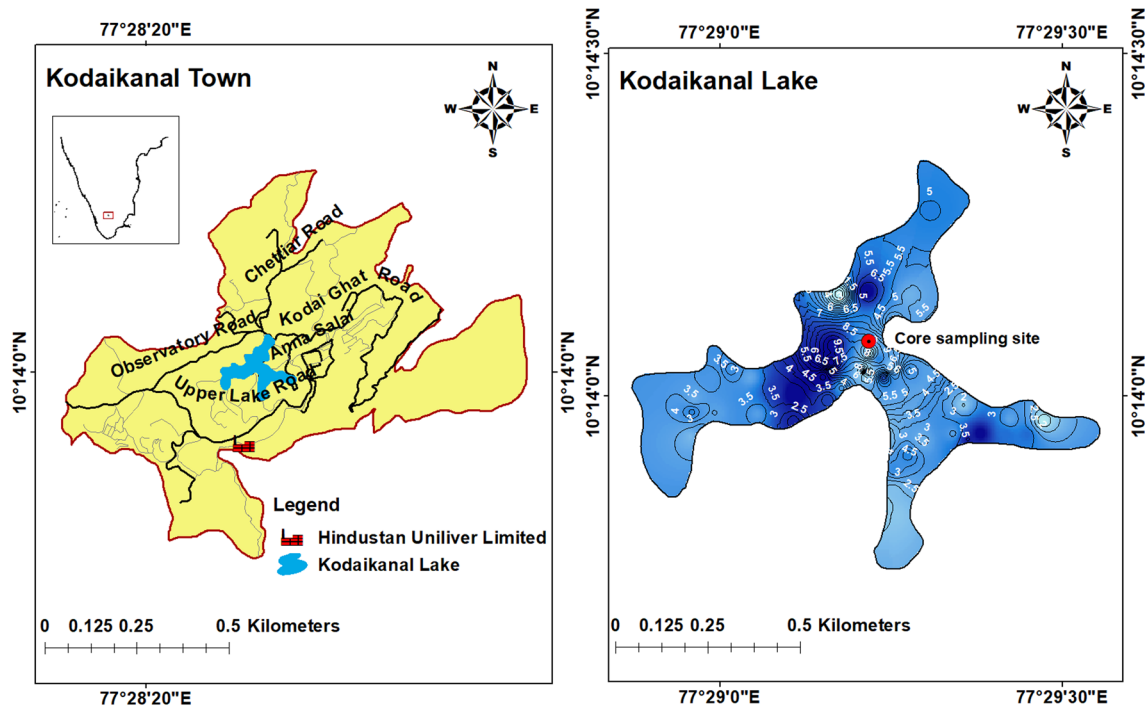


**Fig. 1** Location and bathymetry map of the Kodaikanal Lake

interpolated a raster surface using GPS points. When modeling bathymetry, inverse distance weighting (IDW) interpolation was used; this uses known (adjacent) measured depths to estimate unknown depth data (Bedient and Huber 1992; Burrough and McDonnell 1998).

### Core sampling and analytical procedures

For this study, a sediment core was recovered from the Kodaikanal Lake (E 77.48691 and N 10.23406). The sampling site was chosen based on a bathymetry map and the lake's sedimentary environments. The sediment core sample was recovered from the lake on May 16, 2016. A sediment core with a diameter of 58 mm, length of 56 cm, and water depth are 3–4 m was obtained utilizing a gravity corer and a hand-operated boat. The core sample was maintained vertically throughout sampling to avoid sediment disturbance in the coring tube. The core sediment was moved to the research facility lab and frozen at 4 °C before being sliced into 2 cm intervals. The physical properties of the sediment sample, such as dry bulk density, water content, and porosity, and the remaining sliced core sections, were dried in an oven at 60 °C for 24 h before being stored in the laboratory for particle size and radioisotope estimations ( $^{210}\text{Pb}$ , and  $^{137}\text{Cs}$ ). Sediment samples were analyzed for  $^{210}\text{Pb}$  and  $^{137}\text{Cs}$  activities at the Nuclear Hydrology Laboratory, National Institute of Hydrology in Roorkee, India.

The amounts of dry bulk density were measured before the samples were dried in an oven at a temperature slightly higher than 100 °C for about 7–8 h prior to many experimental assessments. The weight difference between wet and dry sediment samples is used to calculate the water content based on a percentage of the wet sediment sample's weight. After drying, porosity was calculated as a percentage of the volume of water in the sediment pores to the total volume of the sliced core sample (Kumar et al. 1997; Das and Vasudevan 2021).

The grain size of the sediment was analyzed using a Horiba LA-300 scattering particle size analyzer. The sediment samples were dried at 105°, gently crushed, and sieved at a mesh size of 2 mm. Particle size analysis requires sediment samples to be pretreated with hydrogen peroxide ( $\text{H}_2\text{O}_2$ ) and hydrochloric acid (HCl) to decrease the effect of soluble salt, organic matter, and carbonates for each measurement of 10 mg to 5 g. A lesser quantity of  $\text{NaPO}_3$  (sodium hexametaphosphate) was added to separate the fine sediment particles (Aasif et al. 2018; Balamurugan et al. 2021). Based on the findings, the collected data were standardized to determine the sediment size fraction using the Wentworth grade scale method (Wentworth 1922). The particle size was classified into sand > 62.5 μm to 2 mm, silt > 4 μm to 62.5 μm, and clay > 1 μm to 4 μm.

The radioactivity of the alpha emitter radioisotope  $^{210}\text{Po}$  can determine the amount of  $^{210}\text{Pb}$  radionuclide. The  $^{210}\text{Pb}$  activity is evaluated by  $\alpha$ -counting its granddaughter,  $^{210}\text{Po}$ ,

which is presumed to be in decay series with its parent. The  $\alpha$ -counting of the granddaughter product ( $^{210}\text{Po}$ ) is a standard method. The basic radiochemical procedure, in this case, employs  $^{208}\text{Pb}$  as a yield tracer, draining the sediment samples with deionized water, filtration out the residual solids, and converting them to chloride with concentrated hydrochloric acid (HCl). The final solution is prepared with 0.5 M HCl. Polonium isotopes are unexpectedly deposited on the silver planchette before counting with a silicon (Si) surface barrier detector connected to a multichannel analyzer (MCA) by adding ascorbic acid to the HCl solution. Because the going-to-count time was constant throughout the core sections, the standard counting inaccuracy would be less than 10% in the upper core sections and relatively better in the lower sections (Bhishm Kumar et al. 2007). The Genie-2000 software version 3.2 is in control of the whole operation. The counting time for each sediment sample of the Kodaikanal Lake was 6 h. The analysis was performed in Canberra using an Alpha Analyst-Alpha spectrometer-7200-04.

The  $^{137}\text{Cs}$  activity for each section was measured by gamma-counting the oven-dried core sediment sample with high-purity germanium (HPGe) coupled with a 4096 multi-channel analyzer system. The International Atomic Energy Agency (IAEA) recommends the measurement procedures. The same source-detector geometry and density were used with a  $^{137}\text{Cs}$  standard (IAEA-300). To obtain good statistical accuracy, 10 gm or less of the sliced cores measured  $^{137}\text{Cs}$  activity for about 7200–28,800 s intervals. The detection of the limit of the multichannel analyzer for  $^{137}\text{Cs}$  was 0.25 mBq/g, and the standard counting error in the core sections was less than 10% (Singh et al. 2007). The counting time for each sediment sample of the Kodaikanal Lake was 4 h to determine the activity of  $^{137}\text{Cs}$  at 662 keV. The analysis was performed in Canberra–Gamma-ray spectroscopy GC-3520.

## Sedimentation model

The method has also shown promising results at sites with no uniform accumulation. However, the problem is more challenging to determine an appropriate dating model. Some models, such as constant rate supply (CRS), and constant initial concentration (CIC), make use of chronology or age-depth (Appleby and Oldfield 1978; Robbins 1978). However, the assumption used to apply the CIC model is unrelated to the study's criteria.

The CRS model assumes constant  $^{210}\text{Pb}$  fallout from the atmosphere to ocean or lake water at a continuous rate of supply  $^{210}\text{Pb}$  the sediment. Regardless of sediment accumulation rate variation (Krishnaswamy et al. 1971). According to the formula, the cumulative residual excess  $^{210}\text{Pb}$  activity,  $A_d$ , beneath deposits of age  $t$  varies.

$$A_d = A_0 e^{-\lambda t} \quad (1)$$

where,  $t = \frac{x}{s}$   
So,

$$s = \frac{x}{t} \text{LiangKangkang(2014)} \quad (2)$$

$A_d$  is the unsupported  $^{210}\text{Pb}$  in the core below depth " $d$ ", and  $A_0$  is the entire unsupported  $^{210}\text{Pb}$  below the mud/water interface.

The age of the sediments chronology of depth  $x$  is then given by:

$$t = \frac{1}{\lambda} \ln \frac{A(0)}{A(d)} \quad (3)$$

The CRS model uses a  $^{210}\text{Pb}$  flux configuration while accounting for variations in sediment supply. Consequently, this model is used for most sedimentary basins where sediment fluctuates sensibly due to climatic or anthropogenic variations. The model's applicability was thoroughly discussed using a sediment core from Kodaikanal Lake.

The sedimentation rate was determined for the  $^{137}\text{Cs}$  assessment based on the highest layer of  $^{137}\text{Cs}$ , corresponding to the 1963—time markers. The age of the various strata was determined using the known marker's sedimentation rate (Singh and Vasudevan 2021). Whether the  $^{137}\text{Cs}$  peaks were distributed, increasing or decrease did not affect the place of the  $^{137}\text{Cs}$  peaks in the sediment profile or using the  $^{137}\text{Cs}$  peaks as time indicators (Zapata 2002; Zhang et al. 2012; Cheng et al. 2019). The following equation was used to calculate the  $^{137}\text{Cs}$ -derived rate of sedimentation for a sample:

$$r = \frac{H}{n - Y} \quad (4)$$

where  $r$  is the sample's sedimentation rate (cm/yr),  $H$  is the  $^{137}\text{Cs}$  peak depth (cm) at time marker  $Y$  (1963 or 1986), and  $n$  is the sampling year. As a result, the deposited layers can be expressed above the depths of 1963 and 1986 (Cheng et al. 2019; Das and Vasudevan 2021).

$$T_n = Y + \left( \frac{H - h_n}{r} \right) \quad (5)$$

where  $T_n$  and  $h_n$ , respectively, represent the layer's age (year) and depth (cm).

Cheng et al.(2019) suggested a formula for the layers that accumulate below the time marker's depth. The age was determined using the following formula:

$$T_0 = Y - \left( \frac{h_0 - H}{r} \right) \quad (6)$$

where  $T_0$  and  $h_n$ , respectively, represent the layer's age (year) and depth (cm).

where  $L_u$  is the lake's useful life (year),  $D_m$  is the lake's mean depth (m), and  $R_s$  is the rate of sedimentation (cm/year).

### Computation of lake life

The lake life estimate gives an idea of the lake's length of time that would no longer be useful for water-related activities. The lakes' limits have been reduced to such an extent by sedimentation that it is unreasonable to expect them to meet the water needs. Assume that the loss of lake capacity is occurring rapidly; this activity should be performed regularly to understand the lake's situation and create suitable assumptions for lake restoration (Singh et al. 2007). The ratio of average lake depth to weighted average sedimentation rate is used to calculate a lake's expected useful life. The useful life of Kodaikanal Lake is calculated as follows:

$$L_u = D_m \times \frac{100}{R_s} \tag{7}$$

### Results and discussion

There is no research on sedimentation rates and historical sediment records in Kodaikanal Lake to use such models. The examined parameters include bathymetry, dry bulk density, porosity, and sediment texture using the CRS model in a vertical concentration profile of  $^{210}\text{Pb}$ . In addition, the  $^{137}\text{Cs}$  dating technique was used to examine the use of  $^{210}\text{Pb}$  dating models, which were also established by using sediment core samples collected from the lake to comprehend better the accumulation rate, sedimentation rate, and life of the Kodaikanal Lake. The results of the defined data are shown in Tables 1, 2, and 3.

**Table 1** Sand, silt, clay, dry bulk density, porosity and USDA textural classification in Kodaikanal Lake core sediments

Depth in 2 cm	Sand%	Silt%	Clay%	Dry bulk density (g/cm <sup>3</sup> )	Porosity%	USDA textural classification
1	62.62	35.55	1.83	0.77	71.09	Sandy loam
2	56.05	41.71	2.24	0.76	71.20	Sandy loam
3	59.51	37.84	2.65	0.79	70.29	Sandy loam
4	57.50	40.49	2.01	0.63	76.08	Sandy loam
5	58.51	39.66	1.82	0.84	68.19	Sandy loam
6	67.02	30.98	2.00	0.67	74.73	Sandy loam
7	65.98	30.73	3.29	0.59	77.56	Sandy loam
8	60.16	37.39	2.45	0.57	78.63	Sandy loam
9	61.57	36.62	1.81	0.66	74.93	Sandy loam
10	57.37	38.65	3.98	0.71	73.05	Sandy loam
11	62.86	35.22	1.92	0.66	74.97	Sandy loam
12	63.43	34.34	2.23	0.79	70.26	Sandy loam
13	59.22	38.86	1.92	0.63	76.21	Sandy loam
14	58.22	38.83	2.95	1.05	60.33	Sandy loam
15	63.02	34.86	2.12	0.84	68.15	Sandy loam
16	67.05	30.73	2.22	0.76	71.40	Sandy loam
17	68.40	28.10	3.49	0.68	74.38	Sandy loam
18	64.22	33.47	2.30	0.63	76.20	Sandy loam
19	69.62	28.03	2.35	0.59	77.88	Sandy loam
20	68.90	29.29	1.81	0.80	69.64	Sandy loam
21	65.79	32.22	1.99	0.80	69.83	Sandy loam
22	67.61	30.19	2.20	0.91	65.73	Sandy loam
23	69.21	28.62	2.17	0.72	72.73	Sandy loam
Min	56.05	28.03	1.81	0.57	60.33	
Max	69.62	41.71	3.98	1.05	78.63	
Mean	63.21	34.45	2.34	0.73	72.32	

**Table 2** Analyzing data using CRS model to calculate the age dating, mean sedimentation rate and estimation of lake life

Depth (cm)	$^{210}\text{Pb}_{\text{exc}}$ (Bq/kg)	Mass flux(kg/m <sup>2</sup> )	Inventory $^{210}\text{Pb}_{\text{exc}}$ (Bq/m <sup>2</sup> )	Cumulative $^{210}\text{Pb}_{\text{exc}}$ (Bq/m <sup>2</sup> )	Estimated year (year)	Date (AD)	Accumulation rate (kg/m <sup>2</sup> /y)	Sedimentation rate (cm/y)	Estimated lake life (years)
1	9.19±1.19	6.12	56.22	614.26	3.09	2016	1.98±0.17	0.32±0.03	650±24
3	8.9±1.05	5.14	45.75	558.04	5.84	2013	1.87±0.16	0.51±0.05	
6	11.2±1.20	4.59	51.42	512.29	9.24	2010	1.35±0.12	0.65±0.14	
9	14.2±1.36	5.85	83.13	460.88	15.63	2007	0.92±0.09	0.58±0.11	
12	11.2±1.32	5.66	63.36	377.75	21.54	2000	0.96±0.11	0.56±0.12	
15	15.4±1.6	4.66	71.79	314.39	29.87	1994	0.56±0.06	0.50±0.07	
18	4.85±0.8	7.23	35.08	242.60	34.89	1986	1.44±0.15	0.52±0.08	
21	4.94±0.7	4.64	22.93	207.52	38.66	1981	1.23±0.11	0.54±0.09	
24	4.32±0.6	5.05	21.84	184.59	42.71	1977	1.25±0.12	0.56±0.09	
27	5.02±0.9	5.05	25.34	162.75	48.15	1973	0.93±0.11	0.56±0.11	
30	5.82±1.02	4.85	28.25	137.41	55.55	1968	0.66±0.08	0.54±0.1	
33	4.32±0.6	6.12	26.43	109.16	64.47	1960	0.69±0.08	0.51±0.08	
36	4.25±0.4	5.14	21.85	82.73	74.32	1952	0.52±0.03	0.48±0.06	
39	4.14±0.3	4.59	19.01	60.88	86.36	1942	0.38±0.01	0.45±0.04	
42	4.09±0.1	5.85	23.94	41.88	113.63	1930	0.21±0.01	0.37±0.05	
45	3.89±0.1	4.61	17.93	17.93					
Min	3.89±0.1						0.21±0.01	0.32±0.03	
Max	15.4±1.6						1.98±0.17	0.65±0.14	
Mean	7.23±0.86						1.00±0.094	0.51±0.12	

**Table 3** Analyzing data using  $^{137}\text{Cs}$  to calculate the age dating, mean sedimentation rate and estimation of lake life

Depth (cm)	$^{137}\text{Cs}$ (Bq/kg)	Marker years	Mean sedimentation rate (cm/y)		Date (AD)	Estimated Year (Y)	Estimated lake life (years)
			From 1963	From 1986			
1	8.4±0.72	1963 and 1986	0.54	0.53	2015	1	582.75±19
2	11.94±0.9				2013	3	
3	14.93±1.21				2011	5	
7	3.5±0.1				2004	12	
10	6.2±0.48				1998	18	
13	5.8±0.10				1993	23	
16	18.68±1.36				1987	29	
18	12.9±1.11				1983	33	
20	8.4±0.69				1980	36	
23	6.2±0.3				1974	42	
26	12.04±1.1				1969	47	
29	22.04±1.4				1963	53	
33	14.93±1.18				1956	60	
36	11.2±0.84				1950	66	
39	14.2±1.12				1944	72	
40	9.2±0.8				1943	73	
42	8.1±0.6				1939	77	
45	7.9±0.54				1933	83	

Mean sedimentation rate 0.53

### Bathymetry

The bathymetry map of the lake showed the highest and average depths of 11 and 3.38 m, respectively (Fig. 1). The central portion of the water body is also more profound, with more than 5.2 m of water depth compared to its other parts. The surface and catchment areas of the lake are 0.24 km<sup>2</sup> and 4.9 km<sup>2</sup>. The compass bearing of the direction of the major axis of the lake lies in the east–west direction. A shoreline (or) shore is defined as the fringe of land at the edge of a water body that is influenced by the topography of the surrounding landscape: the water-encouraged erosion and estimated 4.34 km of the lake. A contour line represents a corresponding imaginary line on the bottom of a water body with the same elevation or depth along its entire length. The contour line length of the lake is 2.97 km, and the valued contour line lengths are utilized to compute the slope. The distributional pattern of the slope in the lake exhibits gentle slope nature on all four sides, and the central part of the lake shows steep slope nature. In the central portion of the lake, most of the sediments have been deposited at relatively high levels. The steep slopes of the Kodaikanal Lake are the primary factor in influencing increases in the sedimentation rate.

### Dry bulk density

Table 1 shows the result of determining the core sediment, dry bulk density, and porosity. The maximum and minimum dry bulk density ranged from 0.57 to 1.05 g/cm<sup>3</sup> (mean of 0.73 g/cm<sup>3</sup>), with the weight percentage of porosity collected in sediment samples ranging from 60.33 to 78.63 wt.% (mean of 72.32 wt.%). Overall, there was statistical variation in the core depth fractions, dry bulk density, and porosity (Fig. 2). The dry bulk density of the sediment increases as the core depth increases, while the porosity decreases. The observed increase in dry bulk density may be due to sediment consolidation or compaction caused by the weight of the upper sediment layer (overburden pressure).

### Sediment texture

Table 1 shows the sediment grain size determined by this study and the sand, silt, and clay percentages. The results show that the core sediment samples contain 56.05 to 69.62 wt.% (mean of 63.21 wt.%) sand, 28.03 to 41.71 wt.% (mean of 34.55 wt.%) silt, and 1.81 to 3.98 wt.% (mean of 2.34 wt.%) clay. The core fractions mainly were sand and silt, with clay being significantly less abundant in all sections (Fig. 3). The sediments were also classified using the classification of the United States Department of Agriculture (USDA) (Soil Survey Staff 1999). The sediment texture was valued and the results show that the sediments through the

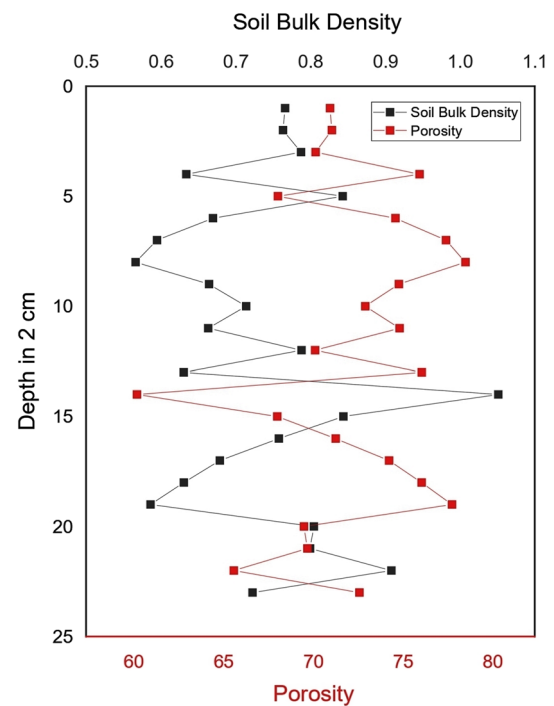


Fig. 2 Dry bulk density and porosity of Kodaikanal Lake sediments

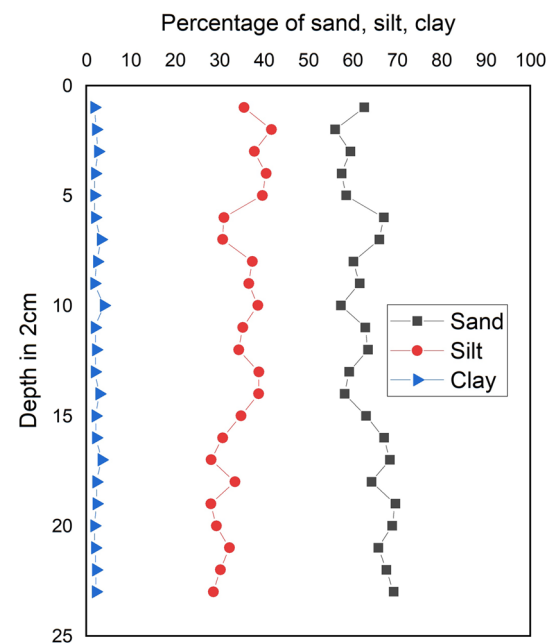
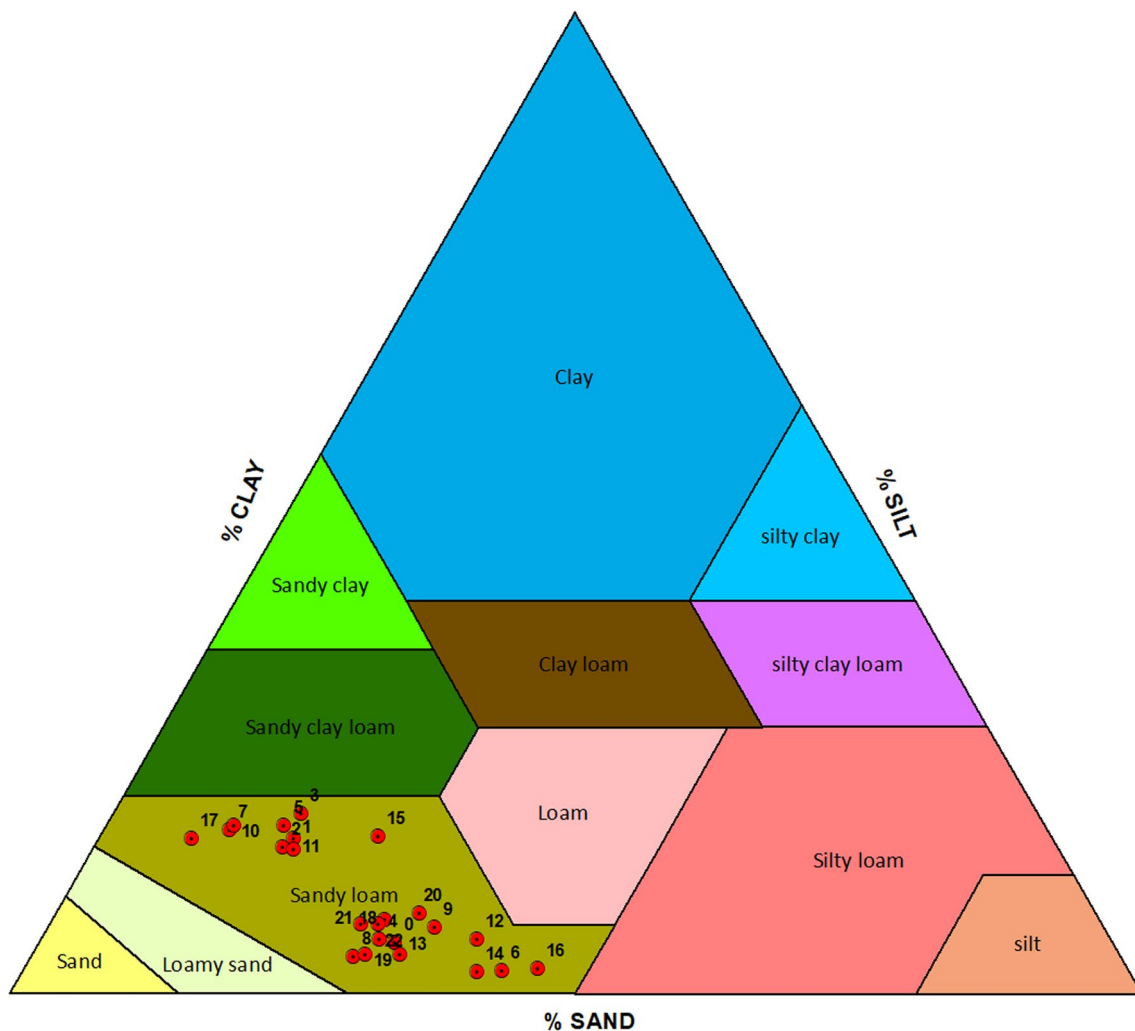


Fig. 3 Sand, silt, and clay percentage of Kodaikanal Lake sediments

lake are typically sandy loam (Fig. 4). The lithology of the sediment core also confirmed this. Deposition of the silt and clay could be transferred to the deepest part, and a coarse (gravel) fraction could be deposited in high-energy shallow lake conditions. The higher catchment gradient and the short



**Fig. 4** Triangular plots for USDA textural classifications of Kodaikanal Lake sediments

distance of sediment transport are also potential natural contributors to silt. The significance of the sedimentation rate at Kodaikanal Lake is mainly due to sediment deposition into the lake through rivers/ streams responsible for accelerating silt inflow into the lake.

### **Vertical concentration profile of $^{210}\text{Pb}$**

The vertical distribution of the  $^{210}\text{Pb}$  concentration was plotted against the core depth of the sediment, which appears in Fig. 5. Table 2 shows that the value of  $^{210}\text{Pb}$  radioactivity ranges from in the core sediment sample  $3.89 \pm 0.1$  to  $15.4 \pm 1.6$  Bq/kg (mean of  $^{210}\text{Pb}$  concentration  $7.23 \pm 0.86$  Bq/ kg). The profile of this sediment core was stair-stepped, with some subsurface peaks and the lowest observed at depths less than 15 cm. The chronological age of any undisturbed sediments at that level is determined by the decrease in  $^{210}\text{Pb}$  with sediment depth.

The sediment profile's upper layer (up to 15 cm) of high activity concentration of  $^{210}\text{Pb}$  was relatively constant, which could be influenced by distribution, bioaccumulation issues, and organism-induced mechanical variations. The presence of settling particles from the atmosphere and land, or older sediment deposits released during resuspension processes, could cause an increase in  $^{210}\text{Pb}$  activity in the core sediment (Miralles et al. 2005; Kumar et al. 2015).

The linear/irregular profile of  $^{210}\text{Pb}$  activity indicates a rapid change in sediment supply and complex hydrodynamics (Andrew et al. 2003). On the other hand, particulate scavenging causes  $^{210}\text{Pb}$  to increase monotonically with depth (Chung et al. 2004). It may also be caused by disruptions in the usual process of sediment supply or surficial sediment combining caused by physical or biological processes. Its silt/sediment load may also impact radionuclide accumulation in the studied area.



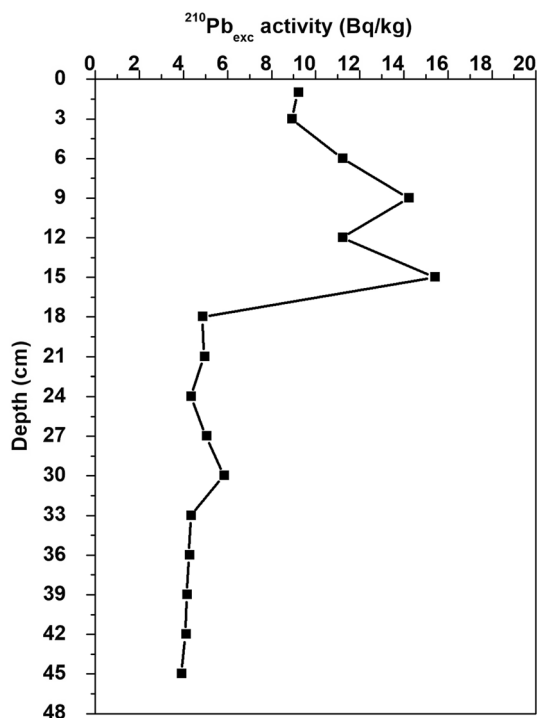


Fig. 5 Depth profile distribution of <sup>210</sup>Pb in Kodaikanal Lake

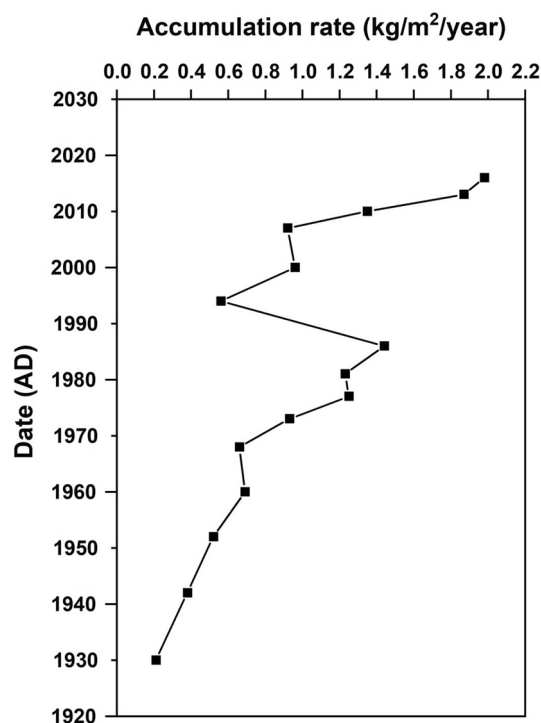


Fig. 6 Accumulation rate using CRS model in Kodaikanal Lake

The assessment of the CRS model for the Kodaikanal Lake core is distinct in Table 2. The estimated accumulation rate range from  $0.21 \pm 0.01$  to  $1.98 \pm 0.17$  kg/m<sup>2</sup>/year (mean of accumulation rate  $1.00 \pm 0.094$  kg/m<sup>2</sup>/year), respectively. The CRS model was used to determine the vertical depth profile of the core sediments from 1902 to 2016 AD and to discuss the increase or decrease in sediment deposition within the lake caused by actions. Figure 6 shows the values gradually accumulated from the bottom to the top of the core sediments. The higher activity of <sup>210</sup>Pb can be attributed to atmospheric fallout from <sup>222</sup>Rn decay, the addition of a considerable amount of rainwater due to heavy rainfall, and preferential accumulation through mud containing fine particles due to industrial activities (Kumar et al. 2015). The accumulation rate of  $0.56 \pm 0.06$  kg/m<sup>2</sup>/year assumes the low accumulation rate and deposition in 1994 AD, representing 15 cm of depth, may be due to deficient rainfall of the catchment area and the desilting of the lake in this period, which makes the deposition process is very low. According to lead dating, 45 cm of the core represents an 86-year-old.

The sedimentation rate in the lake varies between  $0.32 \pm 0.03$  to  $0.65 \pm 0.14$  cm/year (mean of sedimentation rate  $0.51 \pm 0.12$  cm/year). Figure 7 shows the lowest and highest sedimentation rate of Kodaikanal Lake in 2016 and 2010 AD, respectively. This core sediment was separated into three layers; the bottommost layer (onwards 24 cm)

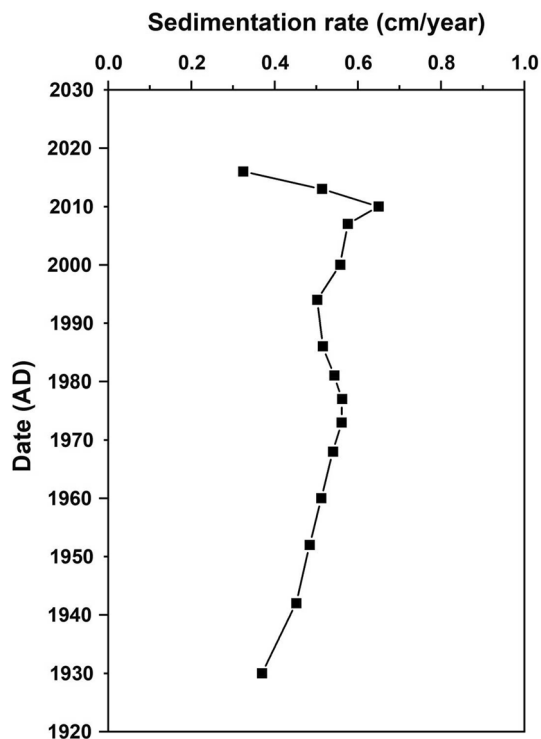


Fig. 7 Sedimentation rate using CRS model in Kodaikanal Lake

gradually increased the sedimentation rate from 1930 up to 1977 AD, with a mean of  $0.50 \pm 0.08$  cm/year. The middle layer of the core sedimentation rate was a more or less similar activity of the environmental condition from 1981 to 2007 AD with a mean of  $0.54 \pm 0.07$  cm/year. The core's recent layer (3 cm and 6 cm) was a higher sedimentation rate in 2010 and 2013 AD ( $0.65 \pm 0.14$  and  $0.51 \pm 0.05$  cm/year), respectively. The highest sedimentation rate is caused mainly by sediment accumulation from the Pambar stream and erosion from the upland area. The CRS model estimated the core sediment sample's mean sedimentation rate as  $0.51 \pm 0.12$  cm/year and the core's age at 86 years (Table 2).

### Vertical concentration profile of $^{137}\text{Cs}$

The  $^{137}\text{Cs}$  radioactivity was measured and ranged from  $3.5 \pm 0.1$  to  $22.04 \pm 1.4$  Bq/kg, with a mean concentration of  $10.92 \pm 0.80$  Bq/kg (Table 3). The measured data are also plotted against the depth of the sediment in Fig. 8. Regarding the vertical distribution of  $^{137}\text{Cs}$ , two distinct peaks are observed; the deeper corresponds to the maximum fallout from nuclear tests (1963), and the upper refers to the Chernobyl accident (1986). Specifically, the sediment core of the upper and lower peaks appears clearly in the depth of 16 and 29 cm with subsequent events of  $18.68 \pm 1.36$  and  $22.04 \pm 1.4$  Bq/kg, respectively (Table 3). Average sedimentation rates were identified by subtracting the depositional depth at the peak by the time elapsed

for the  $^{137}\text{Cs}$  peaks of 1963 and 1986 AD, and ages were assigned based on the obtained mean sedimentation rate (Singhal et al. 2012). Figure 9 shows the vertical profile of  $^{137}\text{Cs}$  activities plotted against date (AD) and two prominent peaks identified in 1963 and 1986 AD. The sedimentation rate employing the 1963 and 1986 AD time markers was assessed to be  $0.54 \pm 0.07$  and  $0.53 \pm 0.07$  cm/year. At the most recent depth of 3 cm, there is a rich sedimentation rate of  $14.9 \pm 31.21$  (2013 AD). This might result from regional phenomena like human activity, regional catchment/limnological processes, and sediment mixing. The overall mean sedimentation rate and age of the  $^{137}\text{Cs}$  core sediment from Kodaikanal Lake have been calculated to be  $0.535 \pm 0.07$  cm/year and 83 years, respectively (Table 3). The results showed that  $^{210}\text{Pb}$  accepted the average sedimentation rate determined by  $^{137}\text{Cs}$  in the profile.

### Computation of lake life

To conclude, consider the calculated sediment accumulation rates in the single zone and the lake's current volume. The useful life of Kodaikanal Lake was calculated by the area-weighted mean sedimentation rate and the lake's mean depth (Singh et al. 2007). The likely life of Kodaikanal Lake, based on an average sedimentation rate of  $^{210}\text{Pb}$  and  $^{137}\text{Cs}$  since 1933, is approximately  $650 \pm 24$  and  $582.75 \pm 19$  years (Tables 2 & 3). Under normal environmental conditions, the lake could be filled if sediment deposition continues at the same rate.

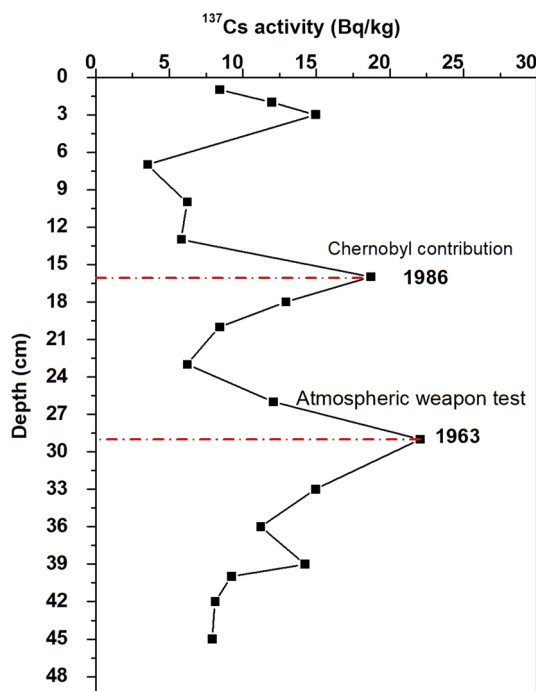


Fig. 8 Depth profile distribution of the  $^{137}\text{Cs}$  in Kodaikanal Lake/

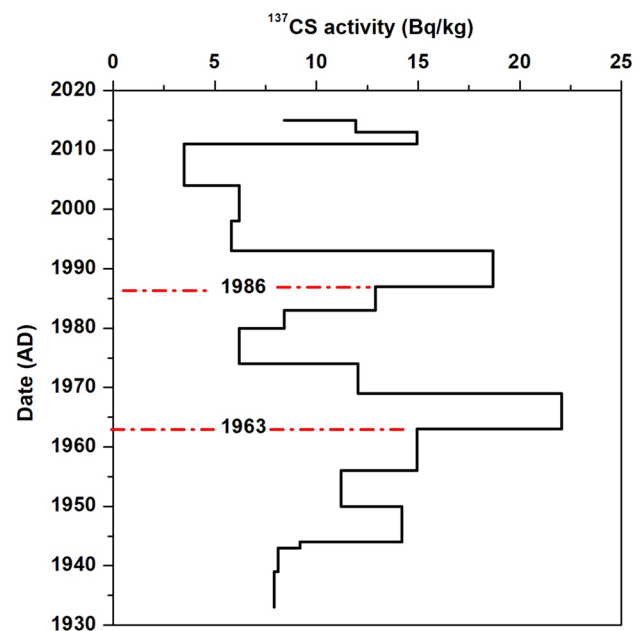


Fig. 9 Depth profile distribution of the  $^{137}\text{Cs}$  activities vs. Date (AD) in Kodaikanal Lake

## Conclusion

Bathymetry is the study of underwater depth, the most important source of information about the lake's morphology. The lake's highest and mean depths are 11 and 3.38 m, respectively. As the core depth increases, the dry bulk density of the sediment increases while the porosity decreases. The core fractions were mainly sand and silt, whereas clay was significantly less abundant. The nature of the sediments is subject to sandy loam. The accumulation rate gradually accumulated from the bottom to the top of the core sediments. The higher activity of  $^{210}\text{Pb}$  can be attributed to atmospheric fallout from  $^{222}\text{Rn}$  decay, the addition of a considerable amount of rainwater due to heavy rainfall, and preferential accumulation through mud containing fine particles due to anthropogenic factors, including industrial activities, agricultural works, deforestation, and civil constructions. The accumulation rate of  $0.56 \pm 0.0.6 \text{ kg/m}^2/\text{year}$  assumes the low accumulation rate and deposition in 1994 AD, representing 15 cm of depth, may be due to deficient rainfall of the catchment area and the sediment desilting to the lake in this period, which makes the deposition process is low in this period.

The sedimentation rate in the lake varied between  $0.32 \pm 0.03$  to  $0.65 \pm 0.14 \text{ cm/year}$ , with a mean sedimentation rate of  $0.51 \pm 0.12 \text{ cm/year}$ . The lake's lowest and highest sedimentation rate was in 2016 and 2010 AD. The highest sedimentation rate at Kodaikanal Lake (downstream reservoirs) is mainly due to sediment inflow through the Pambar stream and erosion from the upland area. The CRS model estimated the mean sedimentation rate in the core sediment sample to be  $0.51 \pm 0.14 \text{ cm/year}$  and the core's age to be 86 years. The sedimentation rate employing the 1963 and 1986 AD time markers was estimated to be  $0.54 \pm 0.07$  and  $0.53 \pm 0.07 \text{ cm/year}$ . The mean sedimentation rate and the age of the Kodaikanal Lake core sediment of  $^{137}\text{Cs}$  have been assessed as  $0.535 \pm 0.07 \text{ cm/year}$  and 83 years, respectively. Therefore, the estimated life of Kodaikanal Lake is approximately  $650 \pm 24$  and  $582.75 \pm 19$  years, based on an average of  $^{210}\text{Pb}$  and  $^{137}\text{Cs}$  sedimentation rates since 1933.

**Acknowledgements** The authors thank the Nuclear Hydrology Laboratory, National Institute of Hydrology in Roorkee, India, for supporting them with this study at various stages. We thank Annamalai University for giving a great opportunity for this research work. In addition, the helpful suggestions of the editors and anonymous reviewers significantly improved the manuscript.

**Funding** The authors gratefully acknowledge the Promotion of University Research and Scientific Excellence (PURSE) and Science and Engineering Research Board (SERB), (Grand No. SR/S4/ES-384/2008 Dated:13/07/2010), Department of Science and Technology, New Delhi, for its financial support in the form of a research grant.

**Data availability** All datasets used or analyzed in this study are available upon request from the lead and corresponding author.

## References

- Aasif M, Chinnamani I, Kumar NS, Hemalatha M, Suresh S (2018) Influence of integrated nutrient management practices on yield and nutrient uptake of rice under system of rice intensification. *Int j Adv* 5(7):10–16
- Al-Masri MS, Mamish S, Budieral Y (2003) Radionuclides and trace metals in eastern Mediterranean Sea algae. *J Environ Radioact* 67(2):157–168. [https://doi.org/10.1016/S0265-931X\(00\)00207-1](https://doi.org/10.1016/S0265-931X(00)00207-1)
- Andrews JT, Giraudeau J (2003) Multi-proxy records showing significant Holocene environmental variability: the inner N. Iceland shelf (Hunafloi). *Quat Sci Rev* 22:175–193
- Appleby PG (2008) Three decades of dating recent sediments by fallout radionuclides: a review. *Holocene* 18(1):83–93. <https://doi.org/10.1177/0959683607085598>
- Appleby PG, Oldfield F (1978) The calculation of lead-210 dates assuming a constant rate of supply of unsupported  $^{210}\text{Pb}$  to the sediment. *CATENA* 5(1):1–8. [https://doi.org/10.1016/S0341-8162\(78\)80002-2](https://doi.org/10.1016/S0341-8162(78)80002-2)
- Appleby PG, Shotyik W, Fankhauser A (1997) Lead-210 age dating of three peat cores in the Jura mountains, Switzerland. *Wat Air Soil Pollut* 100:223–231
- Aycik G, Cetaku D, Erten HN, Salihoglu I (2004) Dating of Black Sea sediments from Romanian coast using natural  $^{210}\text{Pb}$  and fallout  $^{137}\text{Cs}$ . *J Radioanal Nucl Chem* 259(1):177–180
- Balamurugan P, Vasudevan S, Ramkumar T, Selvaganapathi R (2021) An investigation on the assessment of mercury concentration and its spatial distribution in Kodaikanal Lake sediments. *South India Arab J Geosci* 14:1629. <https://doi.org/10.1007/s12517-021-08033-y>
- Baskaran M (2011) Po-210 and Pb-210 as atmospheric tracers and global atmospheric Pb-210 fallout: a review. *J Environ Radioact* 102:500–513
- Baskaran M, Nix J, Kuyper C, Karunakara N (2014) Problems with the dating of sediment cores using excess  $^{210}\text{Pb}$  in a freshwater system impacted by large-scale watershed changes. *J Environ Radioact* 138:355–363
- Bedient PB, Huber WC (1992) *Hydrology and Flood Plain Analysis*, 2nd edn. Addison-Wesley, New York
- Bikit I, Slivka J, Conkic L, Krmar M, Veskovc M, Zikic-Todorovic N, Varga E, Curcic S, Mrdja D (2004) Radioactivity of the soil in Vojvodina (northern province of Serbia and Montenegro). *J Environ Radioact* 78(1):11–19
- Burgherr P, Hirschberg S (2008) A comparative analysis of accident risks in fossil, hydro, and nuclear energy chains. *Hum Ecol Risk Assess* 14(5):947–973
- Burrough PA, McDonnell RA (1998) *Principles of geographical information systems*. Oxford University Press, Oxford
- Butler D (2011) Radioactivity spreads in Japan: fallout is localized, but could persist for years in some regions. *Nature* 471(7340):555–557
- Carter MW, Moghissi AA (1977) Three decades of nuclear testing. *Health Phys* 33(1):55–71
- Cheng Z, Wang XH, Jalon-Rojas I, Liu Y (2019) Reconstruction of sedimentation changes under anthropogenic influence in a medium-scale estuary based on a decadal chronological framework. *Estuar Coast Shelf Sci* 227:106295. <https://doi.org/10.1016/j.ecss.2019.106295>
- Chernobyl Nuclear Accident. [www.iaea.org](http://www.iaea.org), May 14, 2014

- Chino M, Nakayama H, Nagai H, Terada H, Katata G, Yamazawa H (2011) Preliminary estimation of release amounts of  $^{131}\text{I}$  and  $^{137}\text{Cs}$  accidentally discharged from the Fukushima Daiichi nuclear power plant into the atmosphere. *J Nucl Sci Technol* 48(7):1129–1134
- Chung Y, Chang HC, Hung GW (2004) Particulate flux and  $^{210}\text{Pb}$  determined on the sediment trap and core samples from the northern South China Sea. *Cont Shelf Res* 24(6):673–691. <https://doi.org/10.1016/j.csr.2004.01.003>
- Corcoran M, Sherif MI, Smalley C, Li A, Rockne KJ, Giesy JP, Sturchio NC (2018) Accumulation rates, focusing factors, and chronologies from depth profiles of  $^{210}\text{Pb}$  and  $^{137}\text{Cs}$  in sediments of the Laurentian Great Lakes. *J Great Lakes Res* 44(4):693–704. <https://doi.org/10.1016/j.jglr.2018.05.013>
- Das S, Vasudevan S (2021) A comprehensive study on sedimentation rate and sediment age of Satopanth Tal Garhwal Himalaya, using  $^{210}\text{Pb}$  and  $^{137}\text{Cs}$  techniques. *J Radioanal Nucl Chem* 329(2):633–646. <https://doi.org/10.1007/s10967-021-07740-w>
- de Deckere E, De Cooman W, Leloup V, Meire P, Schmitt C, von der Ohe PC (2011) Development of sediment quality guidelines for freshwater ecosystems. *J Soils Sediments* 11(3):504–517. <https://doi.org/10.1007/s11368-010-0328-x>
- Grba N, Krcmar D, Isakovski MK, Jazic JM, Maletic S, Pesic V, Dalmacija B (2016) Priority substances in sediments of the “Carska Bara” special nature reserve, a natural scientific research area on the UNESCO list. *J Environ Manage* 182:149–159. <https://doi.org/10.1016/j.jenvman.2016.07.059>
- Guo J, Costa OS Jr, Wang Y, Lin W, Wang S, Zhang B, Cui Y, Fu H, Zhang L (2020) Accumulation rates and chronologies from depth profiles of  $^{210}\text{Pb}_{\text{ex}}$  and  $^{137}\text{Cs}$  in sediments of northern Beibu Gulf South China Sea. *J Environ Radioact* 213:106136
- HELCOM (2003) The Baltic marine environment 1999–2002. Baltic sea environment proceedings helsinki commission, Helsinki 87:48
- Jeter HW (2000) Determining the ages of recent sediments using measurements of trace radioactivity. *Terra Et Aqua* 78:21–28
- Kirchner G (2011)  $^{210}\text{Pb}$  as a tool for establishing sediment chronologies: examples of potentials and limitations of conventional dating models. *J Environ Radioact* 102(5):490–494. <https://doi.org/10.1016/j.jenvrad.2010.11.010>
- Klaminder J, Appleby P, Crook P, Renberg I (2012) Post-deposition diffusion of  $^{137}\text{Cs}$  in lake sediment: implications for radiocaesium dating. *Sedimentology* 59(7):2259–2267. <https://doi.org/10.1111/j.1365-3091.2012.01343.x>
- Krishnaswamy S, Lal D, Martin JM, Meybeck M (1971) Geochronology of lake sediments. *Earth Planet Sci Lett* 11(1–5):407–414
- Kumar B, Rai SP, Nachiappan RP, Kumar US, Singh S, Diwedi VK (2007) Sedimentation rate in North Indian lakes estimated using  $^{137}\text{Cs}$  and  $^{210}\text{Pb}$  dating techniques. *Curr Sci* 92:10
- Kumar A, Rout S, Karpe R, Mishra MK, Narayanan U, Singhal RK, Tripathi RPM (2015) Inventory, fluxes and residence times from the depth profiles of naturally occurring  $^{210}\text{Pb}$  in marine sediments of Mumbai Harbor Bay. *Environ Earth Sci* 73(8):4019–4031
- Kumar US, Yelgaonkar VN, Navada SV (1997) Radiotracer study on dispersion of sewerage off Mumbai Coast in Western India. Australian Nuclear Association Inc, Sutherland, NSW (Australia) 87–92p
- Last WM, Smol JP (2001) Tracking environmental change using lake sediments: Basin analysis, coring, and chronological techniques. Springer, Dordrecht 1: XXIV 548 <https://doi.org/10.1007/0-306-47671-1>
- McCall PL, Robbins JA, Matisoff G (1984)  $^{137}\text{Cs}$  and  $^{210}\text{Pb}$  transport and geochronologies in urbanized reservoirs with rapidly increasing sedimentation rates. *Chem Geol* 44(1–3):33–65. [https://doi.org/10.1016/0009-2541\(84\)90066](https://doi.org/10.1016/0009-2541(84)90066)
- Miralles J, Radakovitch O, Aloisi JC (2005)  $^{210}\text{Pb}$  sedimentation rates from the northwestern Mediterranean margin. *Mar Geol* 216(3):155–167
- Ritchie JC, McHenry JR (1990) Application of radioactive fallout cesium-137 for measuring soil erosion and sediment accumulation rates and patterns: a review. *J Environ Qual* 2:215–233. <https://doi.org/10.2134/jeq1990.00472425001900020006x>
- Robbins JA, Edgington DN, Kemp AL (1978) Comparative  $^{210}\text{Pb}$ ,  $^{137}\text{Cs}$ , and pollen geochronologies of sediments from Lakes Ontario and Erie. *Quat Res* 10(2):256–278
- Sanders CJ, Santos IR, Silva-Filho EV, Patchineelam SR (2006) Mercury flux to estuarine sediments, derived from Pb-210 and Cs-137 geochronologies (Guaratuba Bay, Brazil). *Mar Pollut Bull* 52(9):1085–1089
- Sanders CJ, Smoak JM, Cable PH, Patchineelam SR, Sanders LM (2011) Lead-210 and Beryllium-7 fallout rates on the southeastern coast of Brazil. *J Environ Radioact* 102(12):1122–1125
- Simon H, Kelemen S, Begy RC (2017) Anthropogenic influences on the sedimentation rates of lakes situated in different geographic areas. *J Environ Radioact* 173:11–17
- Singh KK, Vasudevan S (2021) Reconstruction of sedimentation rates based on the chronological framework of Lake Pykara, Tamil Nadu. *India Environ Monit Assess* 193(7):1–2
- Singh S, Thakural LN, and Kumar B (2007) Estimation of sediment rates and life of Sagar Lake using radiometric dating techniques. *Water Resour Manag* 22(4):443–455
- Singhal RK, Venkatesh M, Wagh DN, Basu H, Chavan T, Pimple MV, and Reddy AVR (2012) Determination of chronological heavy metal deposition and pollution intensity in the bottom sediments of Mumbai Harbour Bay, India using  $^{137}\text{Cs}$  as a tracer. *J Radioanal Nucl Chem* 292(2):863–869
- Sun X, Fan D, Liao H, Liu M, Tian Y, Zhang X, Yang Z (2020) Variation in sedimentary  $^{210}\text{Pb}$  over the last 60 years in the Yangtze River Estuary: New insight to the sedimentary processes. *Mar Geol* 427:106240
- Szczepańska A, Zaborska A, Maciejewska A, Kuliński K, Pempkowiak J (2012) Distribution and origin of organic matter in the Baltic Sea sediments dated with  $^{210}\text{Pb}$  and  $^{137}\text{Cs}$ . *Geochronometria* 39(1):1–9. <https://doi.org/10.2478/s13386-011-0058-x>
- Szarłowicz K, Reczynski W, Czajka A, Spyt B, Szacilowski G (2017) Comprehensive study of the mountainous lake sediments in relation to natural and anthropogenic processes and time (Mały Staw Lake, Poland). *Environ Sci Pollut Res*. 25(4):3335–47
- Szefer P (2002) Metal pollutants and radionuclides in the Baltic Sea—an overview. *Oceanologia* 44(2):129–178
- Tee LT, Ahmad Z, Mohamed CAR (2003) Estimation of sedimentation rates using  $^{210}\text{Pb}$  and  $^{210}\text{Po}$  at the coastal water of Sabah, Malaysia. *J Radioanal Nucl Chem* 256:115–120
- Torabi Kachoozangi F, Karbassi A, Sarang A, Noori R (2020) Sedimentation rate determination and heavy metal pollution assessment in Zariwar Lake. *Iran SN Applied Sciences* 2:1–10
- Tsabarlis C, Kapsimalis V, Eleftheriou G, Laubenstein M, Kaberi H, Plastino W (2012) Determination of  $^{137}\text{Cs}$  activities in surface sediments and derived sediment accumulation rates in Thessaloniki Gulf. *Greece Environ Earth Sci* 67(3):833–843. <https://doi.org/10.1007/s12665-012-1530-5>
- United nations scientific committee on the effects on atomic radiation (UNSCEAR) (2000) Sources and effects of ionizing radiation. UNSCEAR (2000) Report to the General Assembly, with Scientific Annexes, vol I. United Nations, New York
- Walling DE, He Q (1992) Interpretation of caesium-137 profiles in lacustrine and other sediments: the role of catchment-derived inputs. *Hydrobiologia* 235(1):219–30

- Wentworth CK (1922) A scale of grade and class terms for clastic sediments. *J Geol* 5:377–392
- Zapata F (2002) Handbook for the assessment of soil erosion and sedimentation using environmental radionuclides. Kluwer Academic Publishers, pp 219
- Zhang X, Long Y, He X, Wen A, Yan D (2012) Use of  $^{137}\text{Cs}$  and  $^{210}\text{Pb}_{\text{ex}}$  peaks produced by events in the catchment for dating sediments in the Jiulongdian Reservoir, Chuxiong, Yunnan Province China. *IAHS* 356:378–384

**Publisher's Note** Springer Nature remains neutral with regard to jurisdictional claims in published maps and institutional affiliations.

Springer Nature or its licensor (e.g. a society or other partner) holds exclusive rights to this article under a publishing agreement with the author(s) or other rightsholder(s); author self-archiving of the accepted manuscript version of this article is solely governed by the terms of such publishing agreement and applicable law.